

Water extract of *Humulus japonicus* improves age-related cognitive decline by inhibiting acetylcholinesterase activity and the acetylcholine signaling pathway

JU-EUN KIM^{1*}, KYEONG-SEON MIN^{1,2*}, JUN GO¹, HYE-YEON PARK¹, YOUNG-KEUN CHOI¹,
IN-BOK LEE¹, JAEWON SHIN³, HYUN-JU CHO⁴, HONG-SIK KIM⁵, DAE YOUN HWANG²,
WON-KEUN OH³, KYOUNG-SHIM KIM^{1,6} and CHUL-HO LEE^{1,6}

¹Laboratory Animal Resource Center, Korea Research Institute of Bioscience and Biotechnology, Daejeon 34141, Republic of Korea;

²Department of Biomaterials Science, College of Natural Resources and Life Science/Life and Industry Convergence Research Institute, Pusan National University, Miryang, South Gyeongsang 50463, Republic of Korea; ³Korea Bioactive Natural Material Bank,

Research Institute of Pharmaceutical Sciences, College of Pharmacy, Seoul National University, Seoul 08826, Republic of Korea;

⁴NHB Co., Ltd., Seoul 04735, Republic of Korea; ⁵PENS Co., Ltd., Seoul 07206, Republic of Korea; ⁶Department of Functional Genomics, Korea Research Institute of Bioscience and Biotechnology School, University of Science and Technology, Daejeon 34113, Republic of Korea

Received December 24, 2024; Accepted February 21, 2025

DOI: 10.3892/mmr.2025.13496

Abstract. The aging process is associated with a decline in certain cognitive abilities, including learning and memory. This age-related cognitive decline is associated with a reduction in neurogenesis and alterations in the cholinergic system. *Humulus japonicus* (HJ), an ornamental plant in the family *Cannabaceae*, has been reported to exert beneficial effects against neurodegenerative pathophysiologies in mouse models

of disorders such as Alzheimer's and Parkinson's disease. Despite the increasingly aging populations of numerous societies, no study has yet investigated the effects of HJ on cognitive decline associated with normal aging. The present study therefore aimed to examine the protective potential of HJ water (HJW) extract against age-related cognitive decline and scopolamine-induced cognitive impairment. The analyses revealed that the oral administration of HJW markedly improved novel objective recognition and spatial learning in the novel object recognition and Morris water maze tests, respectively, in aged mice. The administration of 600 mg/kg HJW further increased neurogenesis and CA1 thickness in the hippocampi of aged mice. In scopolamine-induced cognitive impairment, administration of 400 or 600 mg/kg HJW markedly increased novel object recognition performance in scopolamine-treated mice. The inhibitory effect of HJW on acetylcholinesterase (AChE) and the activation effects of HJW on the calcium/calmodulin-dependent kinase (CaMK) II α -cAMP response element-binding protein (CREB) and AKT-glycogen synthase kinase-3 β (GSK3 β) pathways were further demonstrated. Overall, these results indicate that HJW administration improves cognitive function through the regulation of AChE activity and CaMKII α -CREB and AKT-GSK3 β pathways.

Correspondence to: Dr Kyoung-Shim Kim or Dr Chul-Ho Lee, Laboratory Animal Resource Centre, Korea Research Institute of Bioscience and Biotechnology, 125 Gwahak-ro, Yuseong, Daejeon 34141, Republic of Korea
E-mail: kskim@kribb.re.kr
E-mail: chullee@kribb.re.kr

*Contributed equally

Abbreviations: ACh, acetylcholine; AChE, acetylcholinesterase; AD, Alzheimer's disease; AKT, protein kinase B; APP, amyloid precursor protein; CA, Cornu ammonis; CaMK, calcium/calmodulin-dependent kinase; ChAT, choline acetyltransferase; CREB, cAMP response element-binding protein; DCX, doublecortin; DG, dentate gyrus; EtOH, ethanol; GSK3 β , glycogen synthase kinase-3 beta; HJ, *Humulus japonicus*; HJE, ethanol extract of *Humulus japonicus*; HJW, water extract of *Humulus japonicus*; LTP, long-term potentiation; MWM, Morris water maze test; NMDA, N-Methyl-d-aspartate; NORT, novel object recognition test; OFT, open field test; PBS, phosphate-buffered saline; PSD95, postsynaptic density protein 95; TBS, tris-buffered saline; UPLC, ultra performance liquid chromatography

Key words: aging, acetylcholine, *Humulus japonicus*, cognitive function, scopolamine-induced model

Introduction

Aging is a complex natural process involving a functional reduction in the activity of various organs, including those of the central nervous system. As the population has aged and life expectancy has increased, the prevalence of cognitive decline has also increased (1-4). Cognitive decline is closely related to neuromorphological changes, including cerebral atrophy, gray and white matter changes, volume loss, ventricular enlargement and sulcus widening (5). Of these, brain atrophy

is associated with age-related neuronal loss, reduced neurogenesis and reduced dendritic branching and spines (6,7).

Acetylcholine (ACh), a major neurotransmitter of the cholinergic system, plays an important role in the nervous system by regulating cerebral cortical development, cortical activity, cognitive performance, learning and memory processes (8) and is also involved in regulating adult hippocampal neurogenesis and neuroplasticity (9,10). The ACh secreted into the synaptic cleft is metabolized into acetyl-CoA and choline by the enzyme acetylcholinesterase (AChE) (11). However, reports have indicated that aged brains have an ACh deficiency at least partially driven by increased AChE activity (12). The neurodegeneration of cholinergic neurons results in the progressive impairment of memory capacity (13,14), which are associated with cognitive decline and neurobehavioral deficits (15-17).

Humulus japonicus (HJ) is a perennial herb found in East Asian countries, including Korea, China and Japan, which has been reported to exert antioxidant and anti-inflammatory effects (18-20). HJ is an annual or perennial climbing herb belonging to the order *Rosales*, family *Cannabaceae*, genus *Humulus* (21). Three other species belong to the genus *Humulus*: *H. japonicus*, *H. lupulus* and *H. yunnansensis* (22). *H. lupulus* has been found to contain a variety of compounds, including essential oils, proteins, lipids and polyphenols (23). The ethanol extract of HJ has been reported to contain neuroprotective components, such as those found in luteolin-7-O-glucoside and apigenin-7-O-glucoside as the most abundant components (24). Methanolic and ethanolic extracts of HJ have previously demonstrated neuroprotective effects by preventing midbrain dopaminergic neuronal death in a mouse model of Parkinson's disease (25). In addition, the methanolic extract of HJ ameliorates Alzheimer's disease (AD) by inhibiting neuroinflammation in the brains of animal models of AD (26). The water extract of HJ (HJW) has also been reported to support the gastrointestinal system (27), promote longitudinal bone growth (28) and exhibit anti-obesity effects (29). However, no study has yet investigated the effects of HJ on cognitive decline associated with normal aging.

In the present study, the chemical constituents of HJ water (HJW) extract were identified using ultra-high-performance liquid chromatography-triple/time-of-flight mass spectrometry (UHPLC-q-TOF-MS/MS). It was subsequently investigated whether HJW improves cognitive function in aged mice using the novel object recognition and Morris water maze tests. The effect of HJW on neurogenesis and AChE activity was subsequently analyzed using immunohistochemistry and an AChE activity colorimetric assay. In addition, the effects of HJW on scopolamine-induced memory impairment and the pathways involved in the regulation of long-term potentiation were further examined. Scopolamine, a muscarinic receptor antagonist, blocks cholinergic neurotransmission and causes memory impairment in mice (30). Scopolamine-induced amnesia is a well-established pharmacological model (31).

Materials and methods

Preparation of the extract. HJW was provided by Neo Health & Beauty (Seoul, Korea) (28). In brief, HJ was extracted in water for 8 h at 90°C. This extract was then filtered,

concentrated using a rotary evaporator at 70°C under reduced pressure and spray dried. The dried extracts were then mixed with dextrin in a 7:3 ratio. Standardized HJW was dissolved in phosphate-buffered saline (PBS) at the concentrations required for *in vitro* and *in vivo* experiments.

UHPLC-q-TOF-MS/MS analysis. A standardized HJW sample was prepared as a test solution by diluting with MeOH to 2 mg/ml. The sample was sonicated at 25°C and 40 kHz for 30 min and centrifuged at 15,000 × g at 4°C for 10 min, and the supernatant was collected. The supernatant was subsequently filtrated through a 0.45 µm filter and further diluted as required for analysis. Ultra-performance liquid chromatography coupled to a quadrupole/time of flight system mass spectrometry² (UPLC-q-TOF-MS/MS) analysis was performed using a Waters Acquity UPLC system (Waters Corporation) coupled to a Waters Xevo F2 qTOF system (Waters Corporation). The analysis was conducted in the scan range of 50-1,500 m/z. A gradient of water and acetonitrile (MeCN) containing 0.1% formic acid was applied as follows: 0-15 min, 18% MeCN; 15-20 min, 18-25% MeCN; 20-25 min, 25% MeCN; 25-30 min, 25-42% MeCN; and 30-35 min, 42% MeCN. The sample injection volume was 10 µl, with a flow rate of 1.0 ml/min during gradient elution. The DAD spectra were recorded at a wavelength of 350 nm. The eluent was directed to a mass spectrometer equipped with an electrospray ionization source and a LockSpray interface (Water ZSpray API; Waters Corporation) for accurate mass analysis.

Animals. To evaluate the efficacy of HJW on age-related cognitive decline caused by aging, young (9 weeks old; weight, 19.9-21.4 g) and aged (18 months old; weight, 23.6-31.8 g) female C57BL/6J mice were used. C57BL/6J mice were purchased from Jackson Laboratory and maintained at the Korea Research Institute of Bioscience and Biotechnology (Daejeon, Korea). To examine the effects of HJW on scopolamine-induced cognitive impairment, male C57BL/6J mice (9 weeks old) were purchased from Daehan BioLink. All mice were housed in plastic cages (25x20x12.5 cm³) and provided with a standard chow diet (cat. no. 2018S; Harlan Teklad) and autoclaved water *ad libitum*. The mice were maintained in a specific-pathogen-free conditions under a 12-h light/dark cycle (lights on at 7:00 AM), with humidity of 50-60% and temperature of 21-22°C.

All animal handling and procedures were performed in accordance with the National Institutes of Health Guide for the Care and Use of Laboratory Animals (32) and were approved by the Institutional Animal Use and Care Committee of the Korea Research Institute of Bioscience and Biotechnology (approval numbers: KRIBB-AEC-23263 for scopolamine-induced cognitive impairment model and KRIBB-AEC-24122 for age-related cognitive impairment model). During the experiment, mice were observed once daily for general health indicators. After completing all experiments, all mice were sacrificed by quick cervical dislocation and their brain were collected and stored at -80°C until use. Death was verified by monitoring the symptoms such as the absence of chest movement, lack of a detectable heartbeat, pale mucous membranes, no response to toe pinch and changes in eye color. Mouse body weight loss >20% was regarded as a humane endpoint in the

present study. None of the experimental animals reached these criteria.

The aged 18-month-old female C57BL/6J mice were divided into four groups: Vehicle-treated (Aged/Vehicle, $n=7$), 200 mg/kg HJW-treated (Aged/HJW200, $n=5$), 400 mg/kg HJW-treated (Aged/HJW400, $n=6$) and 600 mg/kg HJW-treated (Aged/HJW600, $n=7$). Young 9-week-old female C57BL/6J mice were used as controls (Young/Vehicle, $n=9$). The Aged/Vehicle and Young/Vehicle groups were administered PBS, while the Aged/HJW group was treated with HJW five days a week for 12 weeks, continuing until all the experiments were completed. Vehicle and HJW were orally administered using a Zonde needle (cat. no. KN-348-24G-38, Natsume Seisakusho Co., Ltd.). HJW and vehicle were administered five days a week for 12 weeks, continuing until all the experiments were completed. The behavioral experiments were conducted during the 8th and 9th weeks of the experimental period. Behavioral experiments were conducted in the following order: Open field test (OFT), novel object recognition test (NORT) and Morris water maze test (MWM), starting from the eighth week of vehicle or HJW administration. The total of 34 mice were used in this experiment.

Scopolamine-induced cognitive impairment model.

The nine-week-old male C57BL/6J mice were divided into six groups: Vehicle/vehicle-treated (Vehicle/Vehicle, $n=12$), vehicle-scopolamine-treated (Vehicle/Scopolamine, $n=12$), 200 mg/kg HJW/scopolamine-treated (HJW200/Scopolamine, $n=12$), 400 mg/kg HJW/scopolamine-treated (HJW400/Scopolamine, $n=12$) and 600 mg/kg HJW/scopolamine-treated (HJW600/Scopolamine, $n=12$) and 2 mg/kg donepezil/scopolamine-treated (DP2/Scopolamine, $n=10$) groups. Vehicle, HJW and donepezil were orally administered using a Zonde needle and scopolamine was intraperitoneally injected using a 1 ml syringe (Sunshim Medical, Co., Ltd.). A total of 70 mice were used in this experiment, which lasted for 9 days. The behavioral experiment was conducted on days 8 and 9. Donepezil was used as the positive control. During the experimental period, HJW was administered 1 h prior to the behavioral test, while PBS was administered to the vehicle groups. Scopolamine was administered as a single injection at a dose of 1 mg/kg 30 min before the behavioral test on the first day of NORT.

OFT. The locomotor activity of the mice was observed using the OFT (33). Before the start of each test, the floor of the open field chamber was cleaned using 70% ethanol. The mice were carefully removed from their home cage and quickly placed in the center of the open-field chamber. The mice were allowed to explore the open field ($45 \times 45 \times 40$ cm³) for 30 min. Parameters, including the total distance traveled over a 30 min period, were recorded using the SMART video tracking system (Panlab, SL) (34).

NORT. The NORT was performed to assess cognitive function following HJW administration in mice. The mice were habituated to the experimental room for 30 min before the experiment. On the first day, the mice were administered HJW or vehicle 1 h before the experiment. The mice were placed in a rectangular acrylic box ($40 \times 20 \times 20$ cm³) without an object

for 5 min to acclimatize to the box and then returned to their home cage. Subsequently, the mice were placed in a box with two identical objects (wooden cylindrical shape, height: 10 cm, diameter: 2 cm) for 10 min. The following day, one of the familiar objects was changed to a novel object (wooden rectangular pillar shape, $10 \times 2 \times 2.5$ cm³) and the mice were allowed to explore freely for 10 min. During the experiments, the number of touches and sniffing time were analyzed. The preference percentage was calculated using the following formula: [(exploring a novel object or exploring a familiar object)/(exploring a novel object + exploring a familiar object) $\times 100$] (35).

MWMT. Spatial learning and memory were analyzed using the MWMT (36). The apparatus included a pool (diameter, 90 cm; depth, 45 cm) filled with opaque water maintained at 21–23°C. An escape platform (diameter, 10 cm) was placed 1.0–1.5 cm below the water surface in the northwest center. Visual cues were placed at four locations: north, south, east and west. If the mouse did not locate the platform within 30 sec, it was guided to it and allowed to remain there for another 30 sec. Spatial memory was assessed by recording the latency for the animals to escape from the water onto a platform during the learning phase. The mice were subjected to three trials per day for five consecutive days. On the day after the end of the learning phase, mice swam freely in a water pool without the platform for 60 sec. The time and distance in the quadrant and the number of crosses through the platform were recorded using the SMART video tracking system (Panlab, SL) (37–40).

Immunohistochemistry. Brain samples were fixed in 4% paraformaldehyde (w/v) in 0.1 M phosphate buffer (pH 7.2) at 4°C for 3 days and sectioned into 40- μ m coronal sections using a vibratome (cat. no. VT1000S; Leica Microsystems GmbH). Free-floating sections were incubated with 3% H₂O₂ (v/v) in tris-buffered saline (TBS) for 10 min to block endogenous peroxidase activity, washed three times in TBS-T (0.1% Tween 20) and blocked with 2% horse serum (cat. no. 16050130; Thermo Fisher Scientific, Inc.) for 1 h at room temperature. Sections were then incubated overnight at 4°C with a primary antibody against doublecortin (DCX; 1:500; cat. no. SC-8066; Santa Cruz Biotechnology, Inc.), a marker of neurogenesis. Samples were then incubated with the secondary antibody (biotinylated rabbit anti-goat, 1:200; cat. no. BA-5000; Vector Laboratories, Inc.) at room temperature for 1 h. Labelling of biotinylated antibodies was performed using avidin-biotinylated peroxidase complex (Vectastain Elite ABC-HRP Detection Kit; 1:200; cat. no. PK-6100; Vector Laboratories, Inc.) with 3,3'-diaminobenzidine (DAB; cat. no. D8001; MilliporeSigma). Following staining, sections were placed on microscope slides (cat. no. 5116-20F; Muto Pure Chemicals Co., Ltd.) and mounted using Canada balsam (cat. no. C1795; MilliporeSigma). DCX-stained cells in the hippocampus were analyzed using an optical microscope (BX51; Olympus) and MetaMorph (Version 7.7; Molecular Devices Inc.) (26).

Nissl staining. The structural features (Nissl bodies) of neurons and glia were identified using Nissl staining (41). Brain samples fixed in 4% paraformaldehyde were sectioned into 40 μ m coronal sections using a vibratome (Leica

Microsystems GmbH). These sections were then washed three times in TBS-T (0.1% Tween 20) and fixed on slides overnight at room temperature. The sections were hydrated in ethanol from 100-70% and stained with 1% cresyl violet acetate solution (cat. no. C5042; MilliporeSigma) at room temperature for 20 sec. The sections were then rapidly rinsed with distilled water, dehydrated in ethanol from 70-100% and mounted with Canada balsam (MilliporeSigma).

Western blotting. Proteins were extracted from hippocampal tissues using RIPA buffer (cat. no. 20-188; MilliporeSigma) supplemented with a phosphatase inhibitor cocktail (cat. no. 78420; Thermo Fisher Scientific, Inc.). Tissue samples were homogenized using a TissueLyser II (Qiagen GmbH) and centrifuged at 16,600 x g at 4°C for 10 min, after which the supernatant was collected. Protein was quantified using the Bradford assay (cat. no. 5000006; Bio-Rad Laboratories, Inc.). Subsequently, the protein samples were mixed with 5X sample buffer (120 mM Tris-Cl, pH 6.8, 25% glycerol, 5% SDS, 12.5% β -mercaptoethanol and 0.1% bromophenol blue) and boiled at 100°C for 5 min. Protein (15 μ g/lane) was separated on 8-10% SDS-polyacrylamide gels and transferred to a polyvinylidene fluoride membrane (cat. no. 1620117; Bio-Rad Laboratories, Inc.). The membranes were blocked in 5% skimmed milk (cat. no. 232100; Becton, Dickinson and Company) in TBS-T (0.1% Tween 20) and incubated with the primary antibody overnight at 4°C. The primary antibodies were: Actin (cat. no. MAB1501; MilliporeSigma), AKT (cat. no. 9272; Cell Signaling Technology, Inc.), phosphorylated (p-)AKT [Thr308] (cat. no. 9275; CST Biological Reagents Co., Ltd.), calcium/calmodulin-dependent kinase (CaMK) II α (sc-13141; Santa Cruz Biotechnology, Inc.), p-CaMKII α / β (Thr286; sc-12886; Santa Cruz Biotechnology, Inc.), choline acetyltransferase (ChAT; cat. no. 2769; CST Biological Reagents Co., Ltd.), cAMP response element-binding protein (CREB; cat. no. 06-863; MilliporeSigma), p-CREB (Ser133; cat. no. 9198; CST Biological Reagents Co., Ltd.), Gephyrin (cat. no. 147011; Synaptic Systems GmbH), glycogen synthase kinase-3 β (GSK3 β ; cat. no. 9315; CST Biological Reagents Co., Ltd.), p-GSK3 β (Ser9; cat. no. 9336; CST Biological Reagents Co., Ltd.), N-Methyl-d-aspartate (NMDA)R2B (cat. no. 4212; CST Biological Reagents Co., Ltd.), p-NMDAR2B (Tyr1472; cat. no. 4208; CST Biological Reagents Co., Ltd.) and postsynaptic density protein 95 (PSD95; cat. no. 124014, SYSY). The membranes were incubated with horseradish peroxidase-conjugated goat anti-rabbit (cat. no. 111-035-003; Jackson ImmunoResearch Laboratories) or goat anti-mouse (cat. no. 115-035-003; Jackson ImmunoResearch Laboratories) secondary antibodies at room temperature for 1 h. Chemiluminescent signals were developed using EzWestLumi Plus (cat. no. WSE-7120; ATTO Co, Ltd.) and analyzed using Quantity One software (Version 4.66; Bio-Rad Laboratories, Inc.).

Acetylcholinesterase (AChE) activity assay. To investigate the AChE inhibitory activity of HJW, an AChE activity colorimetric assay (ab138871; Abcam) was used. Experiments were performed in accordance with the manufacturer's protocols. In brief, 30 μ l of dilute HJW were added to 96 well plates at concentrations of 0.5, 1.0, 1.5 and 2.0 mg/ml. Donepezil (DP,

cat. no. PHR-1584; MilliporeSigma) at concentrations of 50, 100 and 500 ng/ml was used as the AChE inhibitor-positive control. Subsequently, 10 μ l of AChE was added and mixed well, after which 50 μ l of the reaction mixture was added to each sample. The final volume was adjusted to 100 μ l/well with the AChE assay buffer. The absorbance was measured at 570 nm following incubation at 37°C for 20 min using a Multiskan SkyHigh microplate reader (Thermo Fisher Scientific, Inc.). The percentage of inhibition was calculated by comparing the rates for the sample to the blank (PBS) and control, which contained all components except the tested extract.

To determine AChE activity in mouse brain tissue, we used Ellman's reagent (DTNB; cat. no. D8130; MilliporeSigma). The hippocampi and frontal cortices of male C57BL/6J mice were examined. The brain tissue was homogenized in PBS containing 0.5% Triton X-100 (cat. no. T8787; MilliporeSigma). Following centrifugation at 16,600 x g at 4°C for 10 min, the protein concentration in the supernatant was quantified using the Bradford assay (cat. no. 5000006; Bio-Rad Laboratories, Inc.). Subsequently, 10 μ l of tissue samples were aliquoted into single wells of a 96 well plate, with an equal amount of diluted HJW or donepezil. Subsequently, acetylcholine iodine and DTNB were rapidly added to each well. Plates were then incubated for 20 min at room temperature, protected from light. Absorbance was measured at a wavelength of 412 nm using a Multiskan SkyHigh microplate reader (Thermo Fisher Scientific, Inc.) and AChE inhibition activity is presented as a percentage.

Statistical analysis. Data are expressed as the mean \pm SEM and were analyzed using GraphPad Prism software (version 8.4.3; Dotmatics). The results were analyzed using one-way analysis of variance followed by Tukey-Kramer post hoc tests. Two-sample comparisons were performed using two-tailed Student's t-tests. $P < 0.05$ was considered to indicate a statistically significant difference.

Results

Metabolite analysis of the standardized HJW using UPLC-q-TOF MS/MS spectrometry. The aerial parts of HJ, referred to as 'Yulcho' in Donguibogam, a classic traditional Korean medicine text, have traditionally been used to treat urinary disorders, pneumonia, diarrhea, hypertension and tuberculosis (20,42,43). Although HJW has traditionally been used for these purposes, no comprehensive analysis of the water extracts has been conducted. Therefore, to first establish analytical markers for the standardized HJW, chemical profiling of HJW was conducted using UPLC-qTOF-MS/MS. In the UPLC-qTOF-MS data shown in Fig. 1, 11 peaks in the standardized HJW were analyzed. Seven previously isolated compounds from HJ were used for peak assignments in the chemical profile of standardized HJW (Fig. 1) and four compounds (1, 2, 4 and 5) were predicted based on the molecular weights and MS fragment ion patterns. As a number of studies have identified flavonoid derivatives as the major components of HJ, vitexin (7), luteolin-7-O- β -D-glucopyranoside (8), luteolin (9) and apigenin-7-O- β -D-glucopyranoside (10) were chosen as biomarker substances.

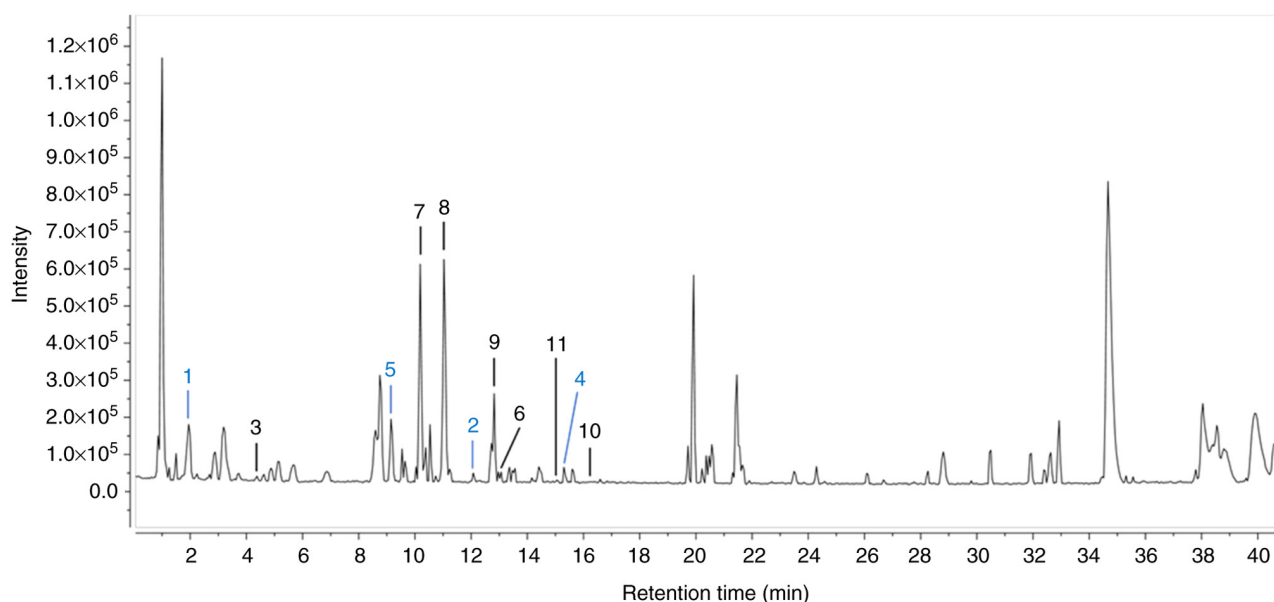


Figure 1. Total ion chromatogram results of the standardized HJW by UPLC-ESI-qTOF-MS/MS spectrometry in the negative ion mode. A total of seven previously isolated compounds underwent peak assignments for the chemical profiling of standard HJW: benzyl- α -L-arabinopyranosyl 1-(1'-6')- β -D-glucopyranoside (3); phenylethyl- α -L-arabinopyranosyl-(1'→6')- β -D-glucopyranoside (6), vitexin (7), luteolin-7-O- β -D-glucopyranoside (8), apigenin-7-O- β -D-glucopyranoside (9), luteolin (10) and apigenin (11). Additionally, four compounds (1, 2, 4 and 5) were predicted based on their molecular weights and MS fragment ion patterns, as follows: Caffeoylquinic acid (1), apigenin-6,8-C-dihexoside (2), apigenin-6-C-glucosyl-8-C-arabinoside (4) and apigenin-6-C-arabinosyl-8-C-glucoside (5). HJW, water extract of *Humulus japonicus*; UPLC-ESI-qTOF-MS/MS, ultra-performance liquid chromatography coupled to a quadrupole/time of flight system mass spectrometry².

Quantitative HPLC-DAD analysis of compounds 7-10. The selectivity, linearity and precision of the analytical method for quantifying the four key marker compounds in HJW were first validated. Selectivity was confirmed by peak purity analysis, ensuring no interference from other compounds, with purity match values exceeding 95% for all markers. Linearity was demonstrated by the high correlation coefficients ($R^2 \geq 0.999$), indicating the proportionality between the concentration and peak areas across the tested ranges. Precision, assessed through relative standard deviation, revealed excellent reproducibility, with values well below 2% for all compounds. These results highlight the robustness and reliability of HPLC for quantifying polyphenolic markers in the standardized HJW.

The retention times of the four marker compounds in HJW were found to be 15.88, 20.76, 25.37. and 33.48 min for vitexin (7), luteolin-7-O- β -D-glucopyranoside (8), luteolin (9) and apigenin-7-O- β -D-glucopyranoside (10), respectively, with respective concentrations of 0.1719, 0.6384, 0.0332 and 0.6384 mg/kg. The standardized HJW contained higher concentrations of luteolin-7-O- β -D-glucopyranoside and apigenin-7-O- β -D-glucopyranoside, as flavonoid glucosides, compared to luteolin. Furthermore, vitexin detected in the HJW was not found in the in 20% ethanol (EtOH) and 70% EtOH extracts of HJ (data not shown).

Effects of HJW on cognitive impairment in aged mice. To determine the protective effect of HJW on age-related cognitive decline, the OFT, NORT and MWMT behavioral tests were conducted (44). The OFT was performed to measure the basal locomotor activity following HJW administration, with results revealing no difference in the total distance traveled between young and aged vehicle- or HJW-treated aged

mice (Fig. 2A). These results indicated that 10 weeks of HJW administration did not affect locomotor activity in aged mice.

The effect of HJW on recognition memory in aged mice was assessed using the NORT. Overall, vehicle-treated young mice showed a significant increase in preference for novel objects in both time and number, whereas vehicle-treated aged mice showed no significant difference in preference for familiar and novel objects in either time or number (Fig. 2B and C). These results indicate the existence of cognitive impairment in aged mice. By contrast, the administration of HJW to aged mice resulted in a significant increase in preference for the novel object in both HJW400 and HJW600 mice (Fig. 2B and C). These results demonstrated that the administration of 400 and 600 mg/kg HJW protected against age-related recognition memory impairment.

The effect of HJW on spatial learning and memory in aged mice was evaluated using the MWMT. In the training trials, there were no significant differences in swimming speed among the groups over five consecutive days (Fig. 3A). The Young/Vehicle group showed a marked decrease in latency on days 4 and 5 compared to day 1 (Fig. 3B). However, the aged/vehicle group showed no obvious differences in the latency between days 1 and day 2-5. Aged/HJW200 group showed a significant decrease in latency from day 3 to 5 compared with that on day 1. The Aged/HJW400 group showed a significant decrease in latency from day 2 compared with day 1 and the Aged/HJW 600 group showed a marked decrease in latency on days 4 and 5 compared with day 1 (Fig. 3B). The probe test revealed no significant differences in swimming speed between the groups (Fig. 3D). However, the time spent in the target quadrant during the probe trial was markedly decreased in the Aged/Vehicle group compared to the Young/Vehicle

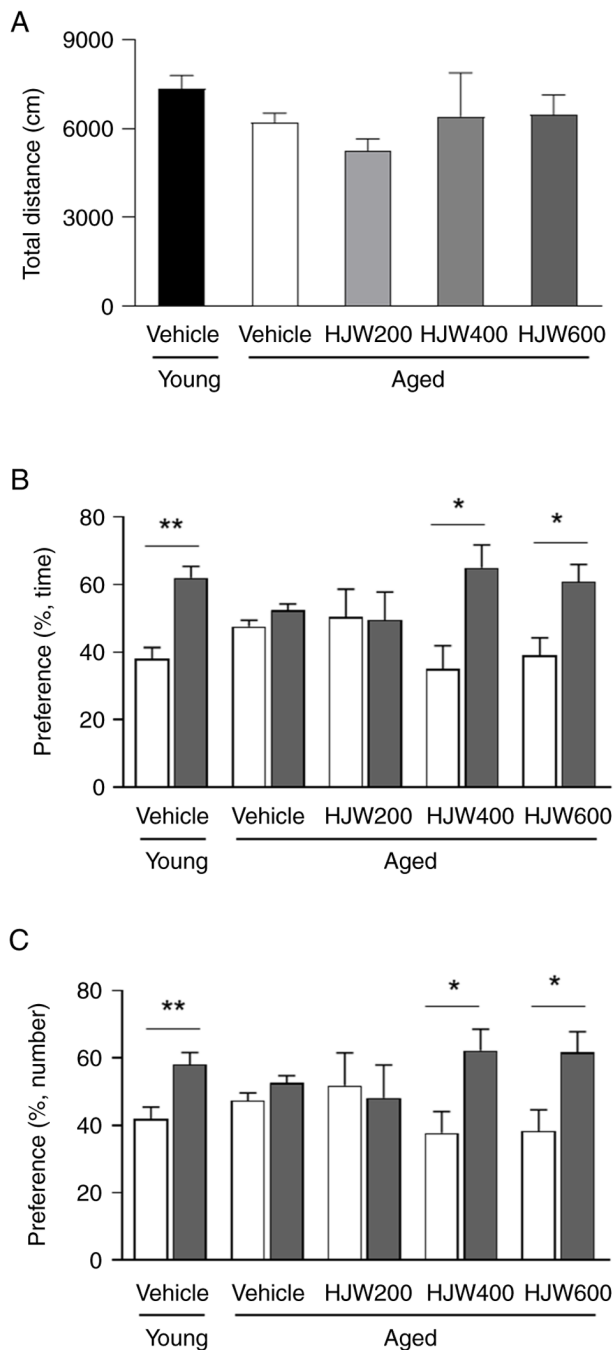


Figure 2. Effects of HJW on locomotor activity and recognition memory in aged C57BL/6J mice. (A) Exploratory locomotion in the open field test for the 30 min test of the total distance moved. (B) Percentage of time spent sniffing and touching the familiar or novel objective for 10 min in the novel object recognition test. (C) Percentage of the number of touches on the familiar or novel objects at 10 min in the novel object recognition test. Young/vehicle group (n=9), Aged/vehicle group (n=7), Aged/HJW200 group (n=5), Aged/HJW400 group (n=10), Aged/HJW600 group (n=10). * $P < 0.05$ and ** $P < 0.01$ vs. Aged/vehicle group. Data are presented as the mean \pm SEM. Statistical analysis was performed using Student's *t*-test. HJW, water extract of *Humulus japonicus*.

group, but not in the HJW-treated Aged group (Fig. 3C). The number of crossings over the platform area was markedly lower in the aged/vehicle group than that in the young/vehicle group; however, this reduction was improved by HJW administration (Fig. 3D), indicating that HJW is effective at reducing the time required to find a platform through spatial perception.

Effects of HJW on neurogenesis in aged mice. To determine the protective effect of HJW against age-related changes in brain morphology, Nissl staining was performed on the hippocampus of aged mice following the administration of either vehicle or HJW (Fig. 4A and B). Notably, Nissl staining showed that HJW administration resulted in a significant increase in CA1 length in the Aged/HJW600 group compared to that in the Aged/Vehicle group, but did not affect CA3 and dentate gyrus (DG) lengths (Fig. 4A and B). Adult hippocampal neurogenesis markedly decreases with age, affecting cognitive function (45) therefore, to determine the effect of HJW on neurogenesis in the brain, hippocampal sections were stained with an antibody against DCX, a specific marker of immature neurons (Fig. 4C). Notably, the Aged/Vehicle group showed almost no DCX-positive cells (0.16 ± 0.16 cells) in the DG of the hippocampus, indicating that adult hippocampal neurogenesis was nearly abolished in aged mice (Fig. 4C and D). The administration of HJW markedly increased the number of DCX-positive cells in aged mice (1.71 ± 0.42 cells) (Fig. 4D). These results indicate that HJW promoted adult hippocampal neurogenesis, which is nearly lost with age.

Inhibitory effects of HJW on AChE activity. To evaluate the inhibitory effect of HJW on AChE, a colorimetric assay of AChE activity was performed. As presented in Fig. 5A, HJW inhibited AChE activity in a dose-dependent manner at various concentrations (0.5, 1.0, 1.5 and 2.0 mg/ml) of HJW, resulting in a reduction of AChE activity of 6.76 ± 0.39 , 12.85 ± 1.21 , 20.26 ± 1.07 and $24.18 \pm 0.58\%$, respectively. Donepezil was used as the positive control (Fig. 5A). The AChE inhibitory activity of HJW in parietal cortical and hippocampal fractions was evaluated using Ellman's method. HJW exhibited AChE inhibition activity at 500 mg/ml in both the hippocampus ($17.0 \pm 2.2\%$) and parietal cortex ($10.0 \pm 4.9\%$), respectively (Fig. 5B and C). These results indicated that HJW possessed AChE inhibitory activity.

HJW improves cognitive ability in scopolamine-induced memory impairment mice. A mouse model of scopolamine-induced memory impairment was used to investigate the effects of HJW on the cholinergic system. The Vehicle/Vehicle group showed a significant preference for the novel object over the familiar object; however, the Vehicle/Scopolamine group showed no difference in preference between familiar and novel objects (Fig. 6A and B). The HJW400/Scopolamine and HJW600/Scopolamine groups both showed markedly improved novel objective recognition memory, showing an increase in the time of sniffing and the number of touches on the novel object (Fig. 6A and B). These results indicated that HJW administration improved scopolamine-induced cognitive impairment.

Effects of HJW on the phosphorylation of NMDAR, CaMKII α and CREB in the hippocampus of scopolamine-induced memory impaired mice. To investigate the effects of HJW on NMDA receptor (NMDAR)-CaMKII α -CREB pathway, western blot analysis was performed in the hippocampus of scopolamine-induced mice. The phosphorylation of NMDAR2B at Tyr1472 was found to be markedly increased in the HJW400/Scopolamine and HJW600/Scopolamine groups

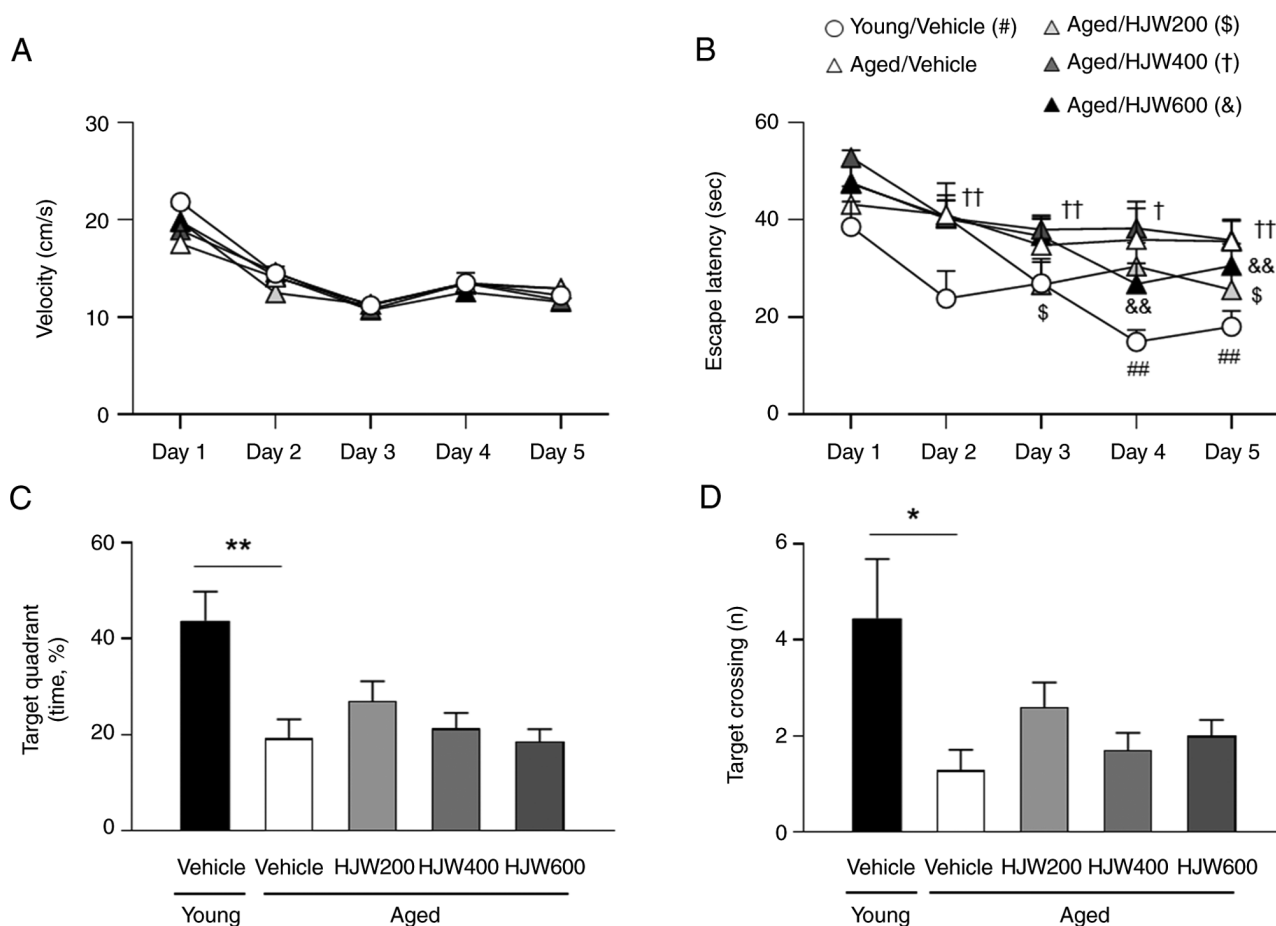


Figure 3. Effects of HJW on spatial learning memory in aged C57BL/6J mice. Results of the Morris water maze test. (A) Swimming speed during the training trials. (B) Latency time to the target platform during the training trials. (C) Percentage of time spent in the target quadrant following removal of the platform (D) The number of target crossings in the platform area. Young/vehicle group (n=9), Aged/vehicle group (n=7), Aged/HJW200 group (n=5), Aged/HJW400 group (n=10), Aged/HJW600 group (n=9). *P<0.05 and **P<0.01 vs. Aged/vehicle group. Data are presented as the mean \pm SEM. Statistical analysis was performed using one-way ANOVA and Student's t-test. HJW, water extract of *Humulus japonicus*.

compared to that in the vehicle/vehicle group (Fig. 7A and B). In addition, the phosphorylation of CaMKII α at Thr286 was markedly increased in all groups administrated with HJW compared with the Vehicle/Vehicle group (Fig. 7A and B). Phosphorylation of CREB at Ser133 was also found to be markedly increased in the HJW400/Scopolamine and HJW600/Scopolamine groups compared to that in the vehicle-only group (Fig. 7A and B). These results suggested that HJW may affect the downstream CREB signaling pathway by regulating CaMKII and NMDAR2B.

Effects of HJW on the phosphorylation of AKT and GSK3 β in the hippocampus of scopolamine-induced memory impaired mice. CREB plays a critical role in cognitive function and hippocampal long-term potentiation (LTP) (46). Several kinases, including AKT and glycogen synthase kinase-3 beta (GSK3 β) are also known to phosphorylate and activate CREB (47). To determine the effects of HJW on the phosphorylation of AKT and GSK3 β , western blotting was performed in the hippocampus of scopolamine-induced model mice. AKT phosphorylation at Thr308 was markedly higher in the HJW200/Scopolamine, HJW400/Scopolamine and HJW600/Scopolamine groups compared to the vehicle-treated group (Fig. 8A and B). The phosphorylation of GSK3 β at Ser9

was also markedly increased in the HJW600/Scopolamine group compared with the Vehicle/Vehicle group (Fig. 8A and B). Furthermore, the effect of HJW on the expression of the synaptic proteins PSD95 and gephyrin in the hippocampus of the scopolamine-treated mouse model was determined by western blot analysis. These results showed that expressions of PSD95, gephyrin and ChAT, the transferase responsible for the synthesis of the neurotransmitter acetylcholine, were not altered by HJW treatment (Fig 8C and D). These results indicated that HJW affects the AKT-GSK3 β signaling pathway, but does not influence the protein expression of PSD95, gephyrin, or ChAT.

Discussion

The present study used 18-month-old female mice to investigate the effects of HJW on age-related cognitive impairment and hippocampal neurogenesis. Chromatographic profiling of the HJW was conducted to reveal its major components, while subsequent *in vivo* analyses demonstrated the protective effects of HJW against age-related cognitive decline in aged mice. The effects of HJW appear to be associated with regulation of neurogenesis, including the modulation of AChE activity and cholinergic signaling.

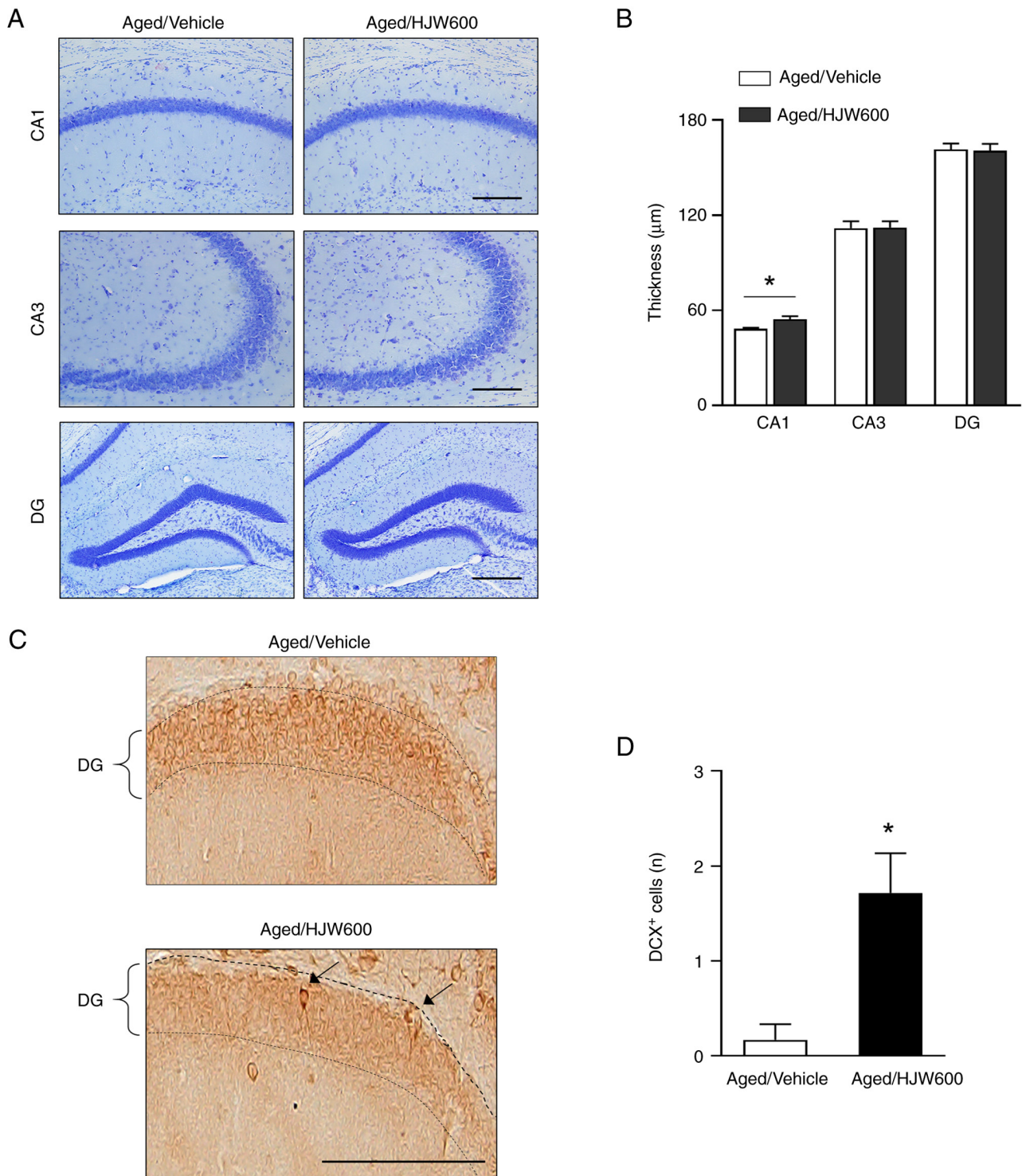


Figure 4. Effects of HJW on neurogenesis in aged C57BL/6J mice. (A) Representative Nissl staining images of the CA1, CA3 and DG hippocampus regions. Scale bar, 200 μm . (B) Quantification of hippocampus layer thickness. (C) Representative DCX-staining images of the hippocampus DG region. Scale bar, 100 μm . (D) Quantification of DCX-positive cells in the DG regions. Aged/vehicle group (n=7) and Aged/HJW600 group (n=9). * $P < 0.05$ vs. Aged/vehicle group. Data are presented as the mean \pm SEM. Statistical analysis was performed using one-way ANOVA. HJW, water extract of *Humulus japonicus*.

The concentration of HJW and age of the mice used were determined based on previous studies (25,26,37,48). Similar to investigations in male mice in a previous study (37), 20-month-old female mice at the start of behavioral experiments showed movement in the OFT comparable to those of 4-month-old young mice. Administration of 200, 400, or 600 mg/kg HJW did not alter locomotor activity in the OFT.

Thus, it appears that HJW did not affect the movement of mice. In the NORT, aged mice were unable to distinguish between familiar and novel objects. However, treatment of aged mice with 400 and 600 mg/kg HJW markedly increased the time and number of instances of novel object recognition in aged mice, indicating an improvement in recognition memory. Furthermore, although there were no significant changes in the

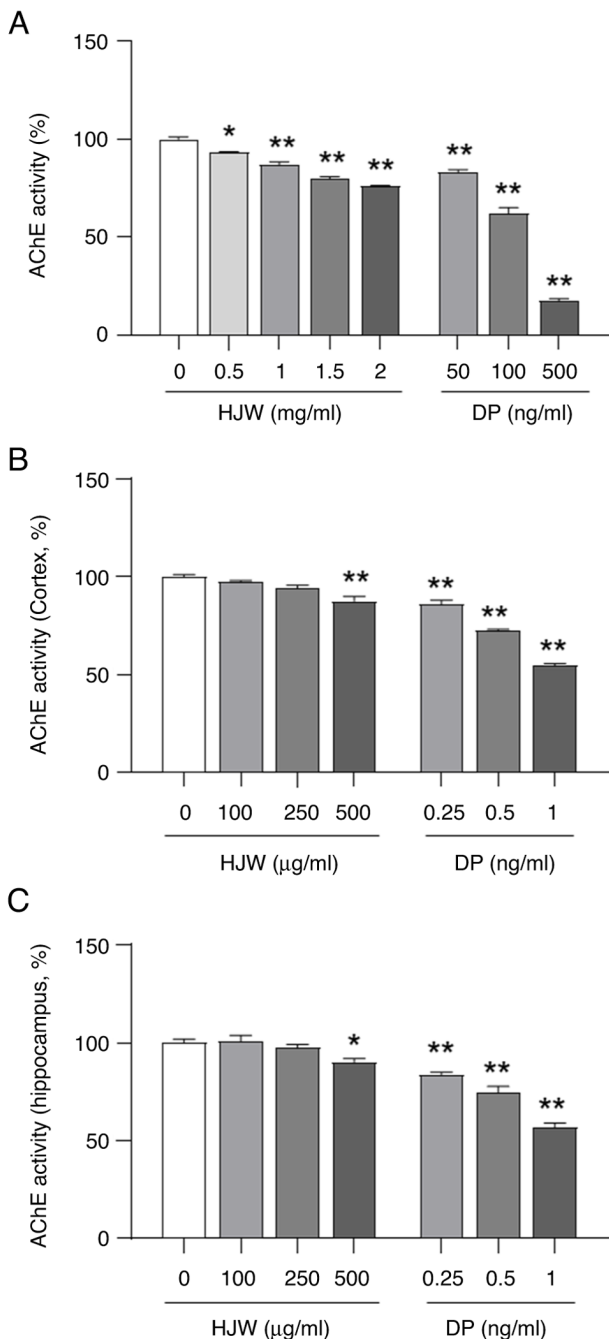


Figure 5. Inhibitory effects of HJW on AChE in C57BL/6J mice. (A) AChE inhibitory effects on HJW. (B) Inhibition of the AChE in the cortex of C57BL/6J mice. (C) Inhibition of the AChE in the hippocampus of C57BL/6J mice *P<0.05 and **P<0.01 vs. control group. Data are presented as the mean ± SEM. Statistical analysis was performed using one-way ANOVA. HJW, water extract of *Humulus japonicus*; AChE, acetylcholinesterase; DP, donepezil.

target crossing and distance in the target quadrant during the probe trial, marked increases were observed in both concentrations compared with the escape time on the first day of the training period in the MWMT, indicating a beneficial effect on spatial learning and memory in aged mice.

Neurogenesis occurs in the hippocampus of the adult brain. The hippocampus is a major brain region involved in learning and memory which is severely affected in AD (49). Newly-formed hippocampal neurons are considered to play

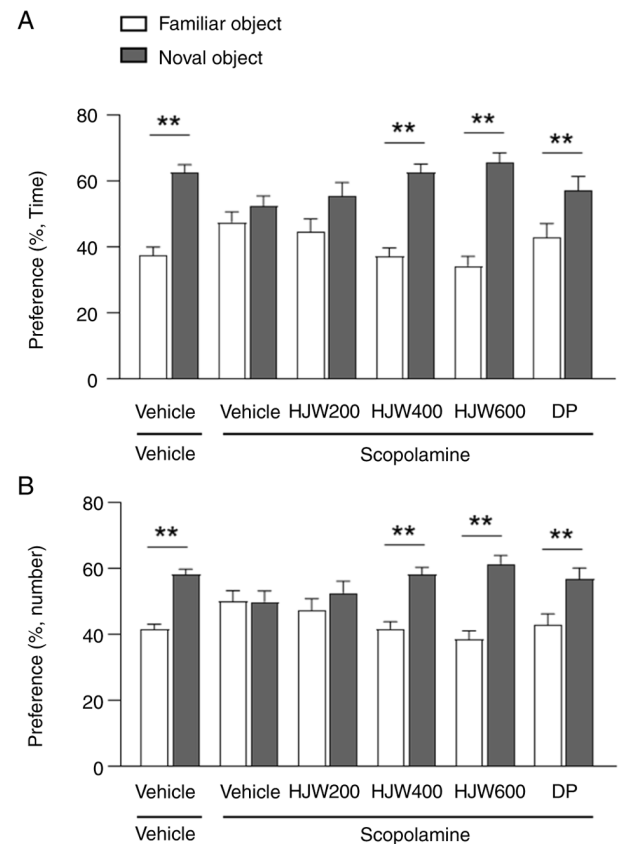


Figure 6. Effects of HJW on recognition memory in scopolamine-induced memory impaired mice. (A) Percentage of time spent sniffing and touching the familiar or novel objectives at 10 min in the novel objective recognition test. (B) Percentage of time spent sniffing and touching the familiar or novel objects for 10 min in the novel objective recognition test. Vehicle/vehicle group (n=12), Vehicle/scopolamine group (n=12), HJW200/scopolamine group (HJW200 mg/kg, n=12), HJW400/scopolamine group (HJW400 mg/kg, n=12) and HJW600/scopolamine group (HJW600 mg/kg, n=10). **P<0.01 vs. Vehicle/scopolamine group. Data are presented as the mean ± SEM. Statistical analysis was performed using Student's t-test. HJW, water extract of *Humulus japonicus*; DP, donepezil.

various roles in learning and memory (50). Neurogenesis declines in aged mice (51), as well as in transgenic animal models of AD (52,53). a number of studies have demonstrated that non-specific positive regulators of neurogenesis, such as environmental enrichment, caloric restriction and physical exercise; as well as pharmacological compounds, such as resveratrol, rapamycin and metformin, stimulate neurogenesis and improve cognitive function in animal models (54). Human neural stem cell transplantation targeting the fimbria-fornix, which is interconnected with the hippocampus, is found to restore cognitive function in an amyloid precursor protein/presenilin-1 murine model of AD (55). DCX is a microtubule-associated protein expressed in postmitotic neurons during migration (56). In the present study, very few neurons were observed in the hippocampi of 21-month-old female mice. However, HJW promoted the regeneration of these cells. Modulation of neurogenesis could help combat cognitive decline and neurodegenerative disorders.

Degeneration of basal forebrain cholinergic neurons, particularly those projecting to the hippocampus, represents an early pathological hallmark of the cognitive deficit

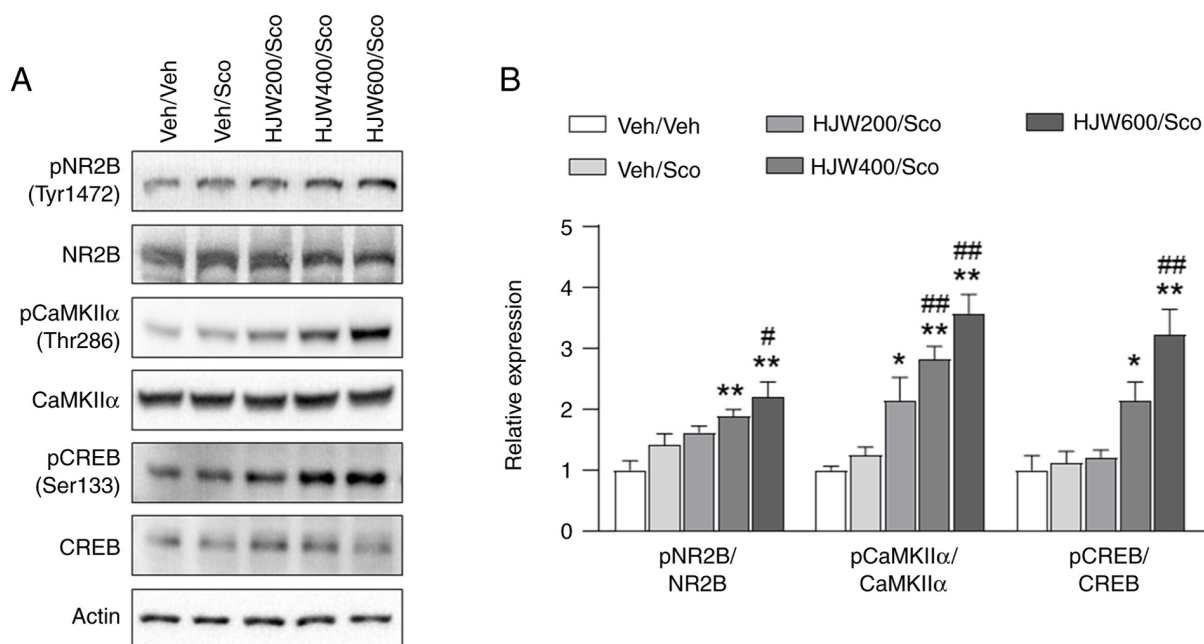


Figure 7. Effects of HJW on the phosphorylation of NR2B, CaMKII α and CREB in the hippocampus of scopolamine-induced mice. Western blot analysis of pNR2B (Tyr1472), NR2B, pCaMKII α (Thr286), CaMKII α , pCREB (Ser133) and CREB. The signal intensities of the bands normalized to actin are shown. (A) A representative western blot image. (B) Quantitative analysis of the NMDA receptor subunit pNR2B (Tyr1472), NR2B, pCaMKII α (Tyr286), CaMKII α , pCREB (Ser133) and CREB. * $P < 0.05$ and ** $P < 0.01$ vs. Vehicle/vehicle group, # $P < 0.05$ and ## $P < 0.01$ vs. Vehicle/scopolamine group. Data are presented as mean \pm SEM. Statistical analysis was performed using one-way ANOVA. HJW, water extract of *Humulus japonicus*; NR2B, NMDA receptor subtype 2B; CaMK, calcium/calmodulin-dependent kinase; CREB, cAMP response element-binding protein; p, phosphorylated; NMDA, N-Methyl-D-aspartate.

characteristic of AD-related dementia (57). Cholinergic neurons have been assumed to undergo moderate degenerative changes during aging, resulting in cholinergic hypofunction, which is related to the progression of memory deficits (58). Moreover, most FDA-approved treatments for dementia aim to enhance cholinergic signaling by inhibiting AChE (59). ACh is known to be involved in the regulation of adult hippocampal neurogenesis (10,60). Neuronal loss within the cholinergic basal forebrain not only leads to cognitive deficits, but also alters the functionality of the DG in adult rats at the cellular level (61). The administration of HJW effectively increased neurogenesis in the DG and inhibited AChE activity. Inhibition of AChE activity is expected to enhance the efficacy of ACh in the brain (62).

Ca²⁺ signaling plays vital roles in various mechanisms of synaptic plasticity at glutamatergic synapses in the hippocampus (63). The enzyme calcium/calmodulin-dependent kinase II (CaMKII) acts as a bridge between calcium signaling and synaptic plasticity and is required for long-term hippocampal potentiation and spatial learning in neurons (64,65). Following the influx of Ca²⁺, Ca²⁺ and calmodulin bind to CaMKII, resulting in the subsequent autophosphorylation at Thr286 in CaMKII α , which plays a critical role in the induction of LTP by integrating Ca²⁺ signals (66). The mutation of Thr286 to alanine in CaMKII α (Camk2 α T286A) disrupts the autophosphorylation of CaMKII, which is crucial for inducing NMDA receptor-dependent LTP in the hippocampus (67). These mutant mice exhibit a lack of NMDA-dependent LTP in the CA1 region of the hippocampus and thus show deficits in spatial learning tasks, such as in the MWM (68). In the 600 mg/kg HJW-treated mice, the autophosphorylation of CaMKII α at Thr286 was markedly increased in the hippocampus, indicating the induction of spine plasticity by

facilitating Ca²⁺ integration. The phosphorylation of CaMKII activates several other transcription factors, including CREB (63). CREB signaling has also been implicated in several neuropathological conditions, including cognitive, aging and neurodegenerative disorders (69).

The chromatographic profile of the ethyl acetate extract of HJ has been reported to contain antioxidant polyphenols including luteolin-7-O- β -D-glucopyranoside, apigenin-7-O- β -D-glucopyranoside, eugenyl- β -D-glucopyranoside, vitexin, luteolin and apigenin (24). In the present study, standardized HJW was used and improvement in cognitive function was observed in an aged mouse model. It is well-established that different solvents used for plant extraction can yield different families of phytochemicals based on the polarity of the solvent used (70). Although the content of each component varies, bioactive compounds, such as flavonoids and phenolics, are extracted using both water and ethyl acetate (70,71). Standardized HJW contains higher concentrations of luteolin-7-O-glucopyranoside and apigenin-7-O-glucopyranoside than luteolin. Furthermore, vitexin detected in the HJW were not found in the 20% EtOH and 70% EtOH extracts of *H. japonicus*. These results partly indicate that, even when comparing flavonoid components, glycosylated compounds with higher polarity in HJW can be extracted more efficiently than their aglycone counterparts.

Previous animal studies have shown that luteolin improves cognitive decline and prevents β -amyloid deposition in the hippocampus in AD (72,73). A beneficial role of apigenin in cognitive and neurobehavioral dysfunction has also been reported (74). One proposed mechanism postulated that luteolin exhibits protective effects on neurological disorders by promoting neurogenesis (75,76). Based on the present results,

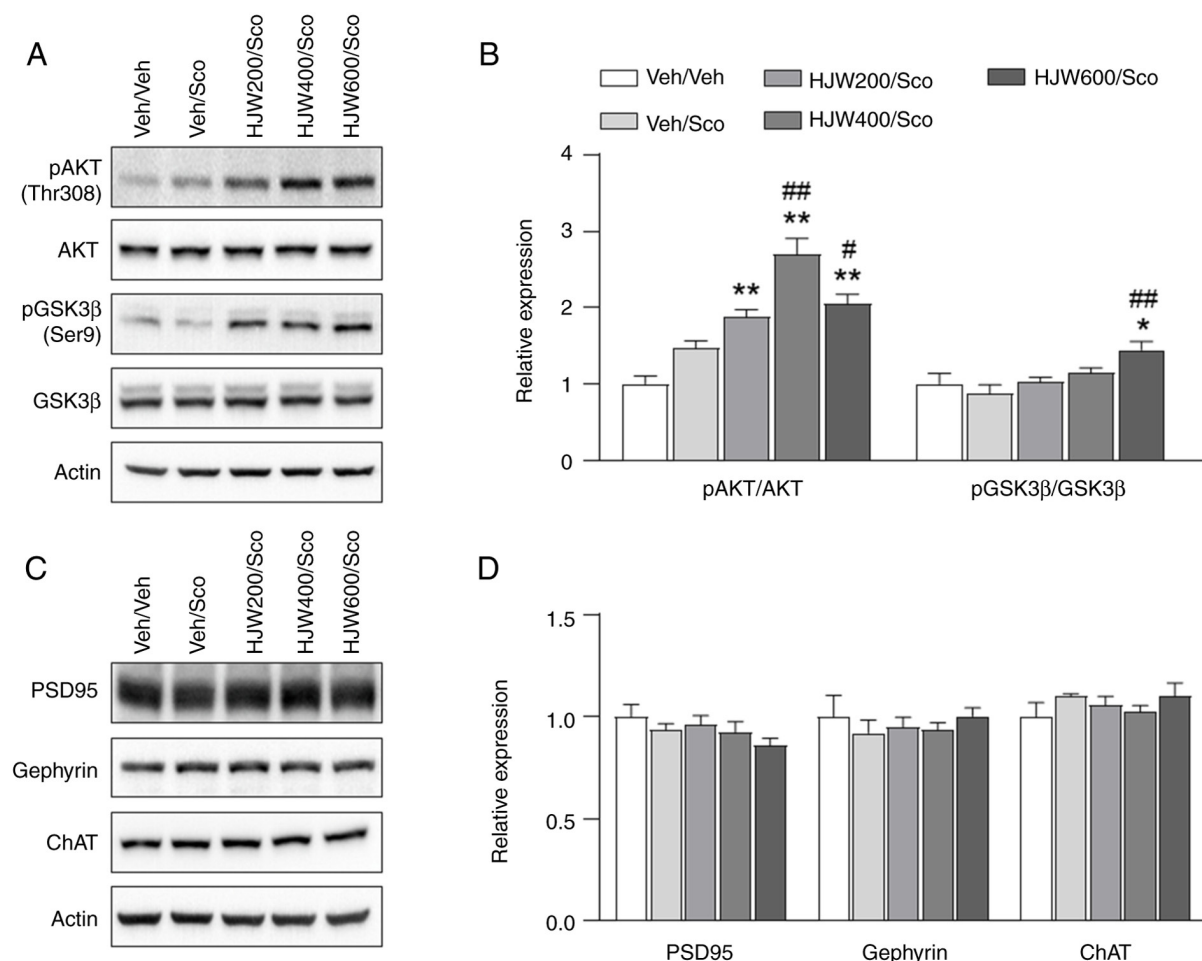


Figure 8. Effects of HJW on the phosphorylation of Akt, GSK3 β and the synaptic marker PSD95, gephyrin, ChAT in the hippocampus of scopolamine-induced mice. Western blot analysis of pAkt (Tyr308), Akt, pGSK3 β (Ser9), GSK3 β , PSD95, gephyrin and ChAT. The signal intensities of the bands normalized to actin are shown. (A) Representative western blot image. (B) Quantitative analysis of pAkt (Tyr308), Akt, pGSK3 β (Ser9) and GSK3 β . (C) Representative western blot image. (D) Quantitative analysis of PSD95, gephyrin and ChAT. * $P < 0.05$ and ** $P < 0.01$ vs. Vehicle/vehicle group, # $P < 0.05$ and ## $P < 0.01$ vs. Vehicle/scopolamine group. Data are presented as the mean \pm SEM. Statistical analysis was performed using one-way ANOVA. HJW, water extract of *Humulus japonicus*; GSK3 β , glycogen synthase kinase-3 beta; ChAT, choline acetyltransferase; p, phosphorylated.

despite the difference in flavonoid content used as a biomarker between the organic solvent and water extracts, standardized HJE showed a beneficial effect on cognitive function in an aging animal model. The present findings are significant because HJW has traditionally been used in oriental medicine and its safety has been well-validated (20,42,43). Nevertheless, before standardized HJE can be used as a functional ingredient for improving cognitive function, further studies are required to elucidate its mechanisms of action and identify the active components responsible for these effects.

The present study found that administering HJW at 600 mg/kg had significant effects on enhancing neurogenesis and cognitive function in aged mice; however, these effects may vary depending on the dosage. Therefore, further research is needed to investigate the effects of different doses on cognitive function and neurobiology to determine the optimal dosing range. Although medicinal herbs are generally considered lower risk than synthetic drugs, they are not entirely free from potential toxicity or adverse effects. There has been increased discussion on the safety assessment of medicinal herbs (77). HJ as a medicinal plant and herb has long been used in traditional medicine for its therapeutic properties (78).

It contains phytochemicals secondary metabolites responsible for their bioactive effects such as alkaloids, flavonoids, tannins and glycosides (79,80). These phytochemicals are known to have pharmacological and toxicological effect contributing their effect on the plants (81). In the food industry, non-toxic and easy-to-handle solvents are preferred for plant extraction (82). Water, being the safest and most cost-effective green solvent, is highly efficient in extracting polar compounds (83). In a previous study, HJW alleviated the high-fat diet-induced obesity and decrease the dyslipidemia profiles; moreover, HJW exhibits a protective effect against liver disease (29). For the development as functional foods, not only is further research on toxicity and safety needed, but also studies on more convenient formulations (such as capsules, tablets, or oral liquids) for large-scale clinical use. In addition, combining HJW with other functional ingredients, such as B vitamins or omega-3 fatty acids, may enhance its overall therapeutic effect (84).

The findings of the present study demonstrated that HJW improved novel object recognition in aged mice as well as in a scopolamine-induced amnesia model, markedly reducing the time spent searching for hidden platforms in aged mice. HJW further enhanced neurogenesis in aged mice and markedly

inhibited AChE activity in the hippocampus and cortex. Mechanistic analyses also indicated that is likely to enhance the phosphorylation of CREB protein, which is important for memory and learning, through increased phosphorylation of the NMDA receptor subtype 2B, CaMKII α , GSK3 β and AKT proteins.

Acknowledgements

Not applicable.

Funding

The present study was supported by the Korea Research Institute of Bioscience and Biotechnology Research Initiative Program (grant nos. KGS1082423 and KGM1312511).

Availability of data and materials

The data generated in the present study may be requested from the corresponding author.

Authors' contributions

JEK and KSM conceptualized and designed the study, performed experiments, analyzed data, and wrote and revised the manuscript. JG, HYP, YKC, IBL, JS, DYH and WKO performed experiments and analyzed data. HJC and HSK supplied the materials and analyzed data. KSK and CHL conceptualized the study, and contributed to the draft and final manuscript. JEK, KSM, KSK and CHL confirm the authenticity of all the raw data. All authors have read and approved the final manuscript.

Ethics approval and consent to participate

All animal experiments were approved by the Institutional Animal Use and Care Committee of the Korea Research Institute of Bioscience and Biotechnology and mouse care and use was in accordance with the National Institutes of Health Guide for the Care and Use of Laboratory Animals (approval nos. KRIBB-AEC-23263 and KRIBB-AEC-24122).

Patient consent for publication

Not applicable.

Competing interests

Hyun-Ju Cho and Hong-Sik Kim are founders of NHB Co. and PENS Co. HJW was supplied by the NHB Co. and PENS Co. The other authors declare that they have no competing interests.

References

- Nicholls LAB, Amanzio M, Guntekin B and Keage H: Editorial: The cognitive ageing collection. *Sci Rep* 14: 10869, 2024.
- Hebert LE, Scherr PA, Bienias JL, Bennett DA and Evans DA: Alzheimer disease in the US population: prevalence estimates using the 2000 census. *Arch Neurol* 60: 1119-1122, 2003.
- Flores G, Flores-Gomez GD, Diaz A, Penagos-Corzo JC, Iannitti T and Morales-Medina JC: Natural products present neurotrophic properties in neurons of the limbic system in aging rodents. *Synapse* 75: e22185, 2020.
- Zaninotto P, Batty GD, Allerhand M and Deary IJ: Cognitive function trajectories and their determinants in older people: 8 years of follow-up in the english longitudinal study of ageing. *J Epidemiol Community Health* 72: 685-694, 2018.
- Blinkouskaya Y and Weickenmeier J: Brain shape changes associated with cerebral atrophy in healthy aging and Alzheimer's disease. *Front Mech Eng* 7: 705653, 2021.
- Chen L, Jiao J and Zhang Y: Therapeutic approaches for improving cognitive function in the aging brain. *Front Neurosci* 16: 1060556, 2022.
- Dickstein DL, Kabaso D, Rocher AB, Luebke JI, Wearne SL and Hof PR: Changes in the structural complexity of the aged brain. *Aging Cell* 6: 275-284, 2007.
- Picciotto MR, Higley MJ and Mineur YS: Acetylcholine as a neuromodulator: Cholinergic signaling shapes nervous system function and behavior. *Neuron* 76: 116-129, 2012.
- Rasmusson DD: The role of acetylcholine in cortical synaptic plasticity. *Behav Brain Res* 115: 205-218, 2000.
- Madrid LI, Jimenez-Martin J, Coulson EJ and Jhaveri DJ: Cholinergic regulation of adult hippocampal neurogenesis and hippocampus-dependent functions. *Int J Biochem Cell Biol* 134: 105969, 2021.
- Mustafab I, Elkamel A, Ibrahim G, Elnashaie S and Chen P: Effect of Choline and acetate substrates on bifurcation and chaotic behavior of acetylcholine neurocycle and Alzheimer's and Parkinson's diseases. *Journal of chemical engineering science* 64: 2096-2112, 2009.
- Moreira EL, de Oliveira J, Nunes JC, Santos DB, Nunes FC, Vieira DS, Ribeiro-do-Valle RM, Pamplona FA, de Bem AF, Farina M, *et al.*: Age-related cognitive decline in hypercholesterolemic LDL receptor knockout mice (LDLr^{-/-}): evidence of antioxidant imbalance and increased acetylcholinesterase activity in the prefrontal cortex. *J Alzheimers Dis* 32: 495-511, 2012.
- Hafez HS, Ghareeb DA, Saleh SR, Abady MM, El Demellawy MA, Hussien H and Abdel-Monem N: Neuroprotective effect of ipriflavone against scopolamine-induced memory impairment in rats. *Psychopharmacology (Berl)* 234: 3037-3053, 2017.
- Blake MG, Krawczyk MC, Baratti CM and Boccia MM: Neuropharmacology of memory consolidation and reconsolidation: Insights on central cholinergic mechanisms. *J Physiol Paris* 108: 286-291, 2014.
- Gasiorowska A, Wydrych M, Drapich P, Zadrozny M, Steczkowska M, Niewiadomski W and Niewiadomska G: The biology and pathobiology of glutamatergic, cholinergic and dopaminergic signaling in the aging brain. *Front Aging Neurosci* 13: 654931, 2021.
- Chen ZR, Huang JB, Yang SL and Hong FF: Role of cholinergic signaling in Alzheimer's disease. *Molecules* 27: 1816, 2022.
- Muller ML and Bohnen NI: Cholinergic dysfunction in Parkinson's disease. *Curr Neurol Neurosci Rep* 13: 377, 2013.
- Go J, Park HY, Lee DW, Maeng SY, Lee IB, Seo YJ, An JP, Oh WK, Lee CH and Kim KS: *Humulus japonicus* attenuates LPS- and scopolamine-induced cognitive impairment in mice. *Lab Anim Res* 38: 21, 2022.
- Kim YB, Kang EJ, Noh JR, An JP, Park JT, Oh WK, Kim YH and Lee CH: *Humulus japonicus* ameliorates irritant contact dermatitis by suppressing NF- κ B p65-dependent inflammatory responses in mice. *Exp Ther Med* 26: 446, 2023.
- Sung B, Chung JW, Bae HR, Choi JS, Kim CM and Kim ND: *Humulus japonicus* extract exhibits antioxidative and anti-aging effects via modulation of the AMPK-SIRT1 pathway. *Exp Ther Med* 9: 1819-1826, 2015.
- McPartland JM: Cannabis systematics at the levels of family, genus and species. *Cannabis Cannabinoid Res* 3: 203-212, 2018.
- Ovidi E, Laghezza Masci V, Taddei AR, Torresi J, Tomassi W, Iannone M, Tiezzi A, Maggi F and Garzoli S: Hemp (*Cannabis sativa* L., Kompolti cv.) and Hop (*Humulus lupulus* L., Chinook cv.) essential oil and hydrolate: HS-GC-MS chemical investigation and apoptotic activity evaluation. *Pharmaceuticals (Basel)* 15: 976, 2022.
- Carbone K and Gervasi F: An updated review of the genus *humulus*: A valuable source of bioactive compounds for health and disease prevention. *Plants (Basel)* 11: 3434, 2022.

24. Lee HJ, Dhodary B, Lee JY, An JP, Ryu YK, Kim KS, Lee CH and Oh WK: Dereplication of components coupled with HPLC-qTOF-MS in the active fraction of humulus japonicus and its protective effects against Parkinson's disease mouse model. *Molecules* 24: 1435, 2019.
25. Ryu YK, Kang Y, Go J, Park HY, Noh JR, Kim YH, Hwang JH, Choi DH, Han SS, Oh WK, *et al*: Humulus japonicus prevents dopaminergic neuron death in 6-hydroxydopamine-induced models of Parkinson's disease. *J Med Food* 20: 116-123, 2017.
26. Park TS, Ryu YK, Park HY, Kim JY, Go J, Noh JR, Kim YH, Hwang JH, Choi DH, Oh WK, *et al*: Humulus japonicus inhibits the progression of Alzheimer's disease in a APP/PS1 transgenic mouse model. *Int J Mol Med* 39: 21-30, 2017.
27. Thein W, Choi WS, Po WW, Khing TM, Jeong JH and Sohn UD: Ameliorative effects of Humulus japonicus extract and polysaccharide-rich extract of Phragmites rhizoma in rats with gastrointestinal dysfunctions induced by water avoidance stress. *Evid Based Complement Alternat Med* 2022: 9993743, 2022.
28. Kim OK, Yun JM, Lee M, Park SJ, Kim D, Oh DH, Kim HS and Kim GY: A mixture of humulus japonicus increases longitudinal bone growth rate in sprague dawley rats. *Nutrients* 12: 2625, 2020.
29. Chung YH, Bang JS, Kang CM, Goh JW, Lee HS, Hong SM, Kim DS, Park ES, Jung TW, Shin YK, *et al*: Aqueous extract of humulus japonicus attenuates hyperlipidemia and fatty liver in obese mice. *J Med Food* 21: 999-1008, 2018.
30. Falsafi SK, Deli A, Hoger H, Pollak A and Lubec G: Scopolamine administration modulates muscarinic, nicotinic and NMDA receptor systems. *PLoS One* 7: e32082, 2012.
31. Kim CY, Seo Y, Lee C, Park GH and Jang JH: Neuroprotective effect and molecular mechanism of [6]-gingerol against scopolamine-induced amnesia in C57BL/6 mice. *Evid Based Complement Alternat Med* 2018: 8941564, 2018.
32. Garber JC, Barbee RW, Beelitzki JT, *et al*: Guide for the care and use of laboratory animals. 8th Edition. National Academies Press, Washington, DC, ppl-246, 2011.
33. Seibenhener ML and Wooten MC: Use of the open field maze to measure locomotor and anxiety-like behavior in mice. *J Vis Exp* 6: e52434, 2015.
34. Shang Q, Chen G, Zhang P, Zhao W, Chen H, Yu D, Yu F, Liu H, Zhang X, He J, *et al*: Myristic acid alleviates hippocampal aging correlated with GABAergic signaling. *Front Nutr* 9: 907526, 2022.
35. Lueptow LM: Novel object recognition test for the investigation of learning and memory in mice. *J Vis Exp*: 55718, 2017.
36. Vorhees CV and Williams MT: Morris water maze: Procedures for assessing spatial and related forms of learning and memory. *Nat Protoc* 1: 848-858, 2006.
37. Go J, Maeng SY, Chang DH, Park HY, Min KS, Kim JE, Choi YK, Noh JR, Ro H, Kim BC, *et al*: Agathobaculum butyriciproducens improves ageing-associated cognitive impairment in mice. *Life Sci* 339: 122413, 2024.
38. Wang DM, Yang YJ, Zhang L, Zhang X, Guan FF and Zhang LF: Naringin enhances CaMKII activity and improves long-term memory in a mouse model of Alzheimer's disease. *Int J Mol Sci* 14: 5576-5586, 2013.
39. Gomez-Oliva R, Martinez-Ortega S, Atienza-Navarro I, Domínguez-García S, Bernal-Utrera C, Geribaldi-Doldán N, Verástegui C, Ezzanad A, Hernández-Galán R, Nunez-Abades P, *et al*: Rescue of neurogenesis and age-associated cognitive decline in SAMP8 mouse: Role of transforming growth factor- α . *Aging Cell* 22: e13829, 2023.
40. Ge W, Ren C, Xing L, Guan L, Zhang C, Sun X, Wang G, Niu H and Qun S: Ginkgo biloba extract improves cognitive function and increases neurogenesis by reducing Abeta pathology in 5xFAD mice. *Am J Transl Res* 13: 1471-1482, 2021.
41. Garcia-Cabezas MA, John YJ, Barbas H and Zikopoulos B: Distinction of neurons, glia and endothelial cells in the cerebral cortex: An algorithm based on cytological features. *Front Neuroanat* 10: 107, 2016.
42. Jang S, Chun JH and Kim KB: Analysis on recent studies trends of humulus japonicus-focusing on research of medical sciences. *J Pediatrics Korean Med* 38: 97-112, 2024.
43. Sun JL, Kim YJ, Cho W, Park SS, Abd El-Aty AM, Mobarak EH, Jung TW and Jeong JH: The extract of humulus japonicus inhibits lipogenesis and promotes lipolysis via PKA/p38 signaling. *Obes Facts* 17: 513-523, 2024.
44. Antunes M and Biala G: The novel object recognition memory: neurobiology, test procedure and its modifications. *Cogn Process* 13: 93-110, 2012.
45. Anacker C and Hen R: Adult hippocampal neurogenesis and cognitive flexibility-linking memory and mood. *Nat Rev Neurosci* 18: 335-346, 2017.
46. Kida S: A functional role for CREB as a positive regulator of memory formation and LTP. *Exp Neurobiol* 21: 136-140, 2012.
47. Wang H, Xu J, Lazarovici P, Quirion R and Zheng W: cAMP response element-binding protein (CREB): A possible signaling molecule link in the pathophysiology of schizophrenia. *Front Mol Neurosci* 11: 255, 2018.
48. Kang CM, Bang JS, Park SY, Jung TW, Kim HC, Chung YH and Jeong JH: The aqueous extract of humulus japonicus ameliorates cognitive dysfunction in Alzheimer's disease models via modulating the cholinergic system. *J Med Food* 25: 943-951, 2022.
49. Anand KS and Dhikav V: Hippocampus in health and disease: An overview. *Ann Indian Acad Neurol* 15: 239-246, 2012.
50. Zhao C, Deng W and Gage FH: Mechanisms and functional implications of adult neurogenesis. *Cell* 132: 645-660, 2008.
51. Kang EJ, Kim JH, Kim YE, Lee H, Jung KB, Chang DH, Lee Y, Park S, Lee EY, Lee EJ, *et al*: The secreted protein Amuc_1409 from Akkermansia muciniphila improves gut health through intestinal stem cell regulation. *Nat Commun* 15: 2983, 2024.
52. Zeng Q, Zheng M, Zhang T and He G: Hippocampal neurogenesis in the APP/PS1/nestin-GFP triple transgenic mouse model of Alzheimer's disease. *Neuroscience* 314: 64-74, 2016.
53. Ding Y, Li L, Wang S, Cao Y, Yang M, Dai Y, Lin H, Li J, Liu Y, Wang Z, *et al*: Electroacupuncture promotes neurogenesis in the dentate gyrus and improves pattern separation in an early Alzheimer's disease mouse model. *Biol Res* 56: 65, 2023.
54. Culig L, Chu X and Bohr VA: Neurogenesis in aging and age-related neurodegenerative diseases. *Ageing Res Rev* 78: 101636, 2022.
55. McGinley LM, Kashlan ON, Bruno ES, Chen KS, Hayes JM, Kashlan SR, Raykin J, Johe K, Murphy GG and Feldman EL: Human neural stem cell transplantation improves cognition in a murine model of Alzheimer's disease. *Sci Rep* 8: 14776, 2018.
56. Gleeson JG, Lin PT, Flanagan LA and Walsh CA: Doublecortin is a microtubule-associated protein and is expressed widely by migrating neurons. *Neuron* 23: 257-271, 1999.
57. Hampel H, Vergallo A, Afshar M, Akman-Anderson L, Arenas J, Benda N, Batrla R, Broich K, Caraci F, Cuello AC, *et al*: Blood-based systems biology biomarkers for next-generation clinical trials in Alzheimer's disease *Dialogues Clin Neurosci* 21: 177-191, 2019.
58. Schliebs R and Arendt T: The cholinergic system in aging and neuronal degeneration. *Behav Brain Res* 221: 555-563, 2011.
59. Anand P and Singh B: A review on cholinesterase inhibitors for Alzheimer's disease. *Arch Pharm Res* 36: 375-399, 2013.
60. Veena J, Rao BS and Srikumar BN: Regulation of adult neurogenesis in the hippocampus by stress, acetylcholine and dopamine. *J Nat Sci Biol Med* 2: 26-37, 2011.
61. Cooper-Kuhn CM, Winkler J and Kuhn HG: Decreased neurogenesis after cholinergic forebrain lesion in the adult rat. *J Neurosci Res* 77: 155-165, 2004.
62. Marucci G, Buccioni M, Ben DD, Lambertucci C, Volpini R and Amenta F: Efficacy of acetylcholinesterase inhibitors in Alzheimer's disease. *Neuropharmacology* 190: 108352, 2021.
63. Zucker RS: Calcium- and activity-dependent synaptic plasticity. *Curr Opin Neurobiol* 9: 305-313, 1999.
64. Rotenberg A, Mayford M, Hawkins RD, Kandel ER and Muller RU: Mice expressing activated CaMKII lack low frequency LTP and do not form stable place cells in the CA1 region of the hippocampus. *Cell* 87: 1351-1361, 1996.
65. Omkumar RV, Kiely MJ, Rosenstein AJ, Min KT and Kennedy MB: Identification of a phosphorylation site for calcium/calmodulin-dependent protein kinase II in the NR2B subunit of the N-methyl-D-aspartate receptor. *J Biol Chem* 271: 31670-31678, 1996.
66. Chang JY, Parra-Bueno P, Laviv T, Szatmari EM, Lee SR and Yasuda R: CaMKII autophosphorylation is necessary for optimal integration of Ca(2+) signals during LTP induction, but not maintenance. *Neuron* 94: 800-808 e4, 2017.
67. Giese KP, Fedorov NB, Filipkowski RK and Silva AJ: Autophosphorylation at Thr286 of the alpha calcium-calmodulin kinase II in LTP and learning. *Science* 279: 870-873, 1998.
68. Sheng M, Thompson MA and Greenberg ME: CREB: A Ca(2+)-regulated transcription factor phosphorylated by calmodulin-dependent kinases. *Science* 252: 1427-1430, 1991.
69. Saura CA and Valero J: The role of CREB signaling in Alzheimer's disease and other cognitive disorders. *Rev Neurosci* 22: 153-169, 2011.

70. Soares MO, Alves RC, Pires PC, Oliveira MB and Vinha AF: Angolan *Cymbopogon citratus* used for therapeutic benefits: nutritional composition and influence of solvents in phytochemicals content and antioxidant activity of leaf extracts. *Food Chem Toxicol* 60: 413-418, 2013.
71. Cieniak C, Walshe-Roussel B, Liu R, Muhammad A, Saleem A, Haddad PS, Cuerrrier A, Foster BC and Arnason JT: Phytochemical comparison of the water and ethanol leaf extracts of the cree medicinal plant, *Sarracenia purpurea* L. (*Sarraceniaceae*). *J Pharm Pharm Sci* 18: 484-493, 2015.
72. Wang H, Wang H, Cheng H and Che Z: Ameliorating effect of luteolin on memory impairment in an Alzheimer's disease model. *Mol Med Rep* 13: 4215-4220, 2016.
73. Liu R, Gao M, Qiang GF, Zhang TT, Lan X, Ying J and Du GH: The anti-amnesic effects of luteolin against amyloid beta(25-35) peptide-induced toxicity in mice involve the protection of neurovascular unit. *Neuroscience* 162: 1232-1243, 2009.
74. Olasehinde TA and Olaokun OO: The beneficial role of apigenin against cognitive and neurobehavioural dysfunction: A systematic review of preclinical investigations. *Biomedicines* 12: 178, 2024.
75. Achour M, Ferdousi F, Sasaki K and Isoda H: Luteolin modulates neural stem cells fate determination: In vitro study on human neural stem cells and in vivo study on LPS-Induced depression mice model. *Front Cell Dev Biol* 9: 753279, 2021.
76. Li HZ, Liu KG, Zeng NX, Wu XF, Lu WJ, Xu HF, Yan C and Wu LL: Luteolin enhances choroid plexus 5-MTHF brain transport to promote hippocampal neurogenesis in LOD rats. *Front Pharmacol* 13: 826568, 2022.
77. Jordan SA, Cunningham DG and Marles RJ: Assessment of herbal medicinal products: Challenges and opportunities to increase the knowledge base for safety assessment. *Toxicol Appl Pharmacol* 243: 198-216, 2010.
78. Petrovska BB: Historical review of medicinal plants' usage. *Pharmacogn Rev* 6: 1-5, 2012.
79. Agidew MG: Phytochemical analysis of some selected traditional medicinal plants in Ethiopia. *Bulletin of the National Research Centre* 46: 87, 2022.
80. Hossain MA and Nagooru MR: Biochemical profiling and total flavonoids contents of leaves crude extract of endemic medicinal plant *Corydalis terminalis* L. Kunth. *Pharma J* 3: 25-30, 2011.
81. Butnariu M, Quispe C, Herrera-Bravo J, Fernández-Ochoa Á, Emamzadeh-Yazdi S, Adetunji CO, Memudu AE, Otlewska A, Bogdan P, Antolak H, *et al*: A review on *Tradescantia*: Phytochemical Constituents, biological activities and health-promoting effects. *Front Biosci (Landmark Ed)* 27: 197, 2022.
82. Proestos C: The benefits of plant extracts for human health. *Foods* 9: 1653, 2020.
83. Plaskova A and Mlcek J: New insights of the application of water or ethanol-water plant extract rich in active compounds in food. *Front Nutr* 10: 1118761, 2023.
84. Oulhaj A, Jerneen F, Refsum H, Smith AD and de Jager CA: Omega-3 fatty acid status enhances the prevention of cognitive decline by B vitamins in mild cognitive impairment. *J Alzheimers Dis* 50: 547-557, 2016.



Copyright © 2025 Kim et al. This work is licensed under a Creative Commons Attribution-NonCommercial-NoDerivatives 4.0 International (CC BY-NC-ND 4.0) License.